Priming xylem for stress recovery depends on coordinated activity of sugar metabolic pathways and changes in xylem sap pH.

(Article begins on next page)

30 August 2024

1 **Priming xylem for stress recovery depends on coordinated activity of sugar metabolic**

2 **pathways and changes in xylem sap pH**

3

4 **Short running title:** How does the biology of xylem apoplast impact the recovery from water

5 stress in poplar?

6

7 Chiara Pagliarani[1,2], Valentino Casolo[3], Maryam Ashofteh Beiragi[1], Silvia Cavalletto[1], Ilenia

8 Siciliano[1,4], Andrea Schubert[1], Maria Lodovica Gullino[1,4], Maciej A. Zwieniecki[5*], Francesca

9 Secchi[1*]

10

11 [1]Department of Agriculture, Forest and Food Science - University of Torino, Largo P. Braccini

12 2, 10095 Grugliasco (Italy)

13 [2]Institute for Sustainable Plant Protection, National Research Council, Strada delle Cacce 73,

14 Torino, Italy

15 [3]Department of Agriculture, Food, Environmental and Animal Sciences, University of Udine,

16 Viale delle Scienze 91, 33100 Udine (Italy)

17 [4]AGROINNOVA, Centre for Innovation in the Agro-Environmental Sector, University of

18 Torino, Largo P. Braccini 2, 10095 Grugliasco (Italy)

19 [5]Department of Plant Sciences, UC Davis, Davis, CA, 95616 (USA)

20

21 *Equal contribution.

22

23 Corresponding author: Francesca Secchi

24   Department of Agricultural, Forest and Food Sciences (DISAFA), University of Torino, Largo

25   Paolo Braccini 2, 10095, Grugliasco (TO), Italy

26   Email: francesca.secchi@unito.it

27

Abstract

In some plant species under low tension, the fast removal of embolism takes place during recovery from drought. However, the functional biology underlying this process still remains elusive.

We subjected poplar trees to drought stress followed by a period of recovery. Water potential, hydraulic conductivity, gas exchange, xylem sap pH and both carbohydrate content in xylem sap and woody stems were monitored in combination with an analysis of carbohydrate metabolism, enzyme activity and expression of candidate genes involved in sugar metabolic and transport pathways.

Drought resulted in an alteration of carbohydrate metabolism and a differential partitioning between starch and soluble sugars. Upon stress, an increase in the starch degradation rate and the overexpression of sugar symporter genes promoted the efflux of disaccharides (mostly maltose and sucrose) to the apoplast. In turn, the efflux activity of the sugar-proton co-transporters caused a drop in xylem pH. The newly acidic environment induced the activity of apoplastic invertases leading to the accumulation of monosaccharides in the apoplast thus providing the main osmoticum necessary for recovery.

During drought and recovery, a complex network of coordinated molecular and biochemical signals was activated at the interface between xylem and parenchyma cells that appeared to prime the xylem for hydraulic recovery.

Keyword index: apoplastic pH, disaccharides, drought, gene expression, monosaccharides, *Populus,* recovery, starch

Introduction

Embolism formation is a physical process influenced by a wide range of factors, including water tension, physical properties of the xylem, chemical properties of xylem sap, temperature and previous plant embolism history (Hacke *et al.*, 2001, Holbrook & Zwieniecki, 1999, Jensen *et al.*, 2016, Stiller & Sperry, 2002, Tyree & Zimmermann, 2002). Under drought stress or periods of high transpirational demand, increasing xylem tension increases the likelihood of embolism formation. Embolism accumulation progressively reduces stem water transport capacity, which can increase leaf water stress, forcing stomatal closure and reducing photosynthetic activity (Brodribb & Jordan, 2008). In the event of severe stress, when water loss by transpiration exceeds the transport capacity of xylem, runaway xylem embolism may occur leading to the complete cessation of water transport and, in the worst-case scenario, plant death (Sperry *et al.*, 1998). Therefore, it is conceivable that any strategy implemented by the plant to hinder and/or minimize the negative effects of embolism, including the restoration of hydraulic transport capacity upon stress relief, could be crucial for guaranteeing plant survival (Barigah *et al.*, 2013, Choat *et al.*, 2012, Tyree & Ewers, 1991).

Mounting experimental evidence proves suggests that during drought recovery a restoration of xylem functionality may occur in several plant species, even when the bulk of water in the xylem remains under low to moderate tension (Brodersen *et al.*, 2010, Nardini *et al.*, 2011, Secchi & Zwieniecki, 2011, Zwieniecki & Holbrook, 2009). Thus, recovery from embolism cannot happen spontaneously and requires the presence of living xylem cells in the proximity of empty vessels to facilitate the process and overcome existing energy gradients. Consequently, both the spatial arrangement and the amount of wood parenchyma could be crucial for successful embolism removal. The majority of living cells in the xylem are located in

4

parenchyma rays, which are often in direct contact with vessels. Parenchyma ray cells provide temporary storage for non-structural carbohydrates (NSC) in the form of sugar and starch (Salleo *et al.*, 2004, Spicer, 2014) and constitute a radial water redistribution pathway; both prerequisite functions that can promote the active repair of embolized conduits. *In vivo* observations show that during recovery, vessels fill up with water (Holbrook *et al.*, 2001, Scheenen *et al.*, 2007) initially derived from water droplets that preferentially form and grow on vessel walls that are in contact with living parenchyma cells (Tyree *et al.,* 1999, Brodersen *et al.*, 2010). However, while direct *in vivo* observations indicate parenchyma cells as important players in the hydraulic restoration process, the functional biology of this process remains unresolved.

According to current active embolism removal models, during water stress, starch in wood parenchyma cells is hydrolyzed to soluble sugars, which are transported along with ions to the apoplast (Secchi & Zwieniecki, 2012). Accumulation of osmotica decreases the apoplastic water potential allowing aquaporin-mediated water entry into the empty vessels upon relief from water stress. Once vessels have been refilled and become functional, sugars and ions are washed away with the transpiration stream (Brodersen & McElrone, 2013, Secchi & Zwieniecki, 2012, Secchi & Zwieniecki, 2016, Zwieniecki & Holbrook, 2009). These models are consistent with observations of NSC accumulation dynamics in parenchyma cells of drought-stressed plants. For instance, embolism presence has been shown to alter carbohydrate metabolism and the partitioning between starch and soluble sugars in xylem parenchyma (Salleo *et al.*, 2009, Secchi & Zwieniecki, 2011, Tomasella *et al.*, 2017) resulting in the accumulation of high levels of NSC content in trees subjected to short-term drought events (Trifilo *et al.*, 2017). Additionally, the ability to recover from embolism has been found to be species-specific and correlated with the concentration of soluble carbohydrates accumulated at the stem level (Savi *et al.*, 2016).

97   Shifts in carbohydrate metabolism during drought stress coincide with changes in

98   apoplastic pH. Alkalization or acidification is one of the first chemical changes observed in the

99   xylem sap of drought-exposed plants (Bahrun *et al.*, 2002, Sharp & Davies, 2009, Sobeih *et al.*,

100   2004) and can trigger the systemic activation of whole-plant water-stress responses (Schachtman

101   & Goodger, 2008). A drop in xylem pH has been observed *in vivo* in poplar stems subjected to

102   water stress (Secchi & Zwieniecki, 2012), and furthermore, *in vitro* analysis associated an acidic

103   apoplastic pH to an increased accumulation of sugars in the xylem sap of poplar stems (Secchi &

104   Zwieniecki, 2016). These observations suggest that the accumulation of sugars in the xylem

105   apoplast is controlled by xylem pH, where a lower pH may induce apoplastic sucrose hydrolysis

106   potentially via acidic invertase activity.

107   The directionality of sucrose symporters is determined by proton (pH) and sucrose

108   concentration gradients across the plasma membrane (Carpaneto *et al.*, 2005). Thus, an increase

109   of cellular sucrose content shifts the concentration gradient and triggers *de novo* efflux of sucrose

110   to the apoplast. In functional vessels, such efflux would be unnoticeable as sugars are continually

111   washed away. However, in embolized vessels, an increase in sucrose concentration, in

112   combination with a lower pH in the xylem apoplast, would induce acidic invertase activity in the

113   walls resulting in an accumulation of monosaccharides (mainly glucose and fructose). Sugar

114   accumulation in the walls would significantly lower their osmotic potential and lay the basis for

115   refilling upon relief from water stress (Secchi & Zwieniecki, 2012, Secchi & Zwieniecki, 2016).

116   According to this model, changes in xylem apoplast chemistry should be coupled to membrane

117   transport and cellular carbohydrate metabolism. We hypothesize that if the response of xylem

118   parenchyma cells to severe stress is a coordinated biological process that results in the priming of

119   xylem for hydraulic recovery, then concurrent changes in xylem pH, sugar composition and

6

120 concentration should be correlated with the expression of genes that affect carbohydrate

121 metabolism and transport. In this study, we confirm that a lower xylem apoplastic pH is linked to

122 carbohydrate accumulation in poplar, and we explore the changes in the transcriptional activity

123 of candidate genes involved in sugar metabolism, transport and partitioning. The present work

124 further supports the notion that severe water stress triggers a set of biological processes priming

125 xylem for embolism removal upon watering (Secchi & Zwieniecki, 2014).

126

127 **Materials and Methods**

128 *Plant material and experimental set up*

129 One-year-old hybrid poplars (*Populus tremula* x *Populus alba* clone 717-1B4) were grown in a

130 glasshouse under partially controlled climatic conditions. The average daily greenhouse

131 temperature was 24.9 ± 5.35°C and relative humidity values ranged between 42.3 and 61.8 %.

132 Maximum photosynthetic photon flux density (PPFD) ranged between 1330 and 1580 µmol

133 photons m^{-2} s^{-1} and 12-h-light/12-h-dark cycles were followed using halogen lamps, when

134 necessary, to supplement light and guarantee a minimum PPFD of 500-600 µmol photons m^{-2}

135 s^{-1}. Each plant grew in a 5 L pot filled with a substrate composed of sandy-loam soil/expanded

136 clay/peat mixture (2:1:1 by weight). A total of 51 hybrid poplars with an average height of 180 ±

137 5 cm and stem diameter at the soil level of 11.6 ± 0.58 mm, were used in this study. The plants

138 were divided into two groups: twenty-four poplars, belonging to group one, were used to

139 estimate the level of embolism in response to water stress (PLC). Those plants were further

140 divided into 3 subgroups: A) six plants watered daily (CTR), B) six plants severely water-

141 stressed by withholding irrigation until the stem water potential (Ψstem) was below -2 MPa

142 (STRESS), and C) twelve plants first stressed to below -2 MPa and then watered (PLC was

143 measured respectively after 1 and 7 days of recovery, REC1-7). The remaining twenty-seven

144 poplars, belonging to the second group, were split into nine irrigated control trees (CTR) that

145 were irrigated to water holding capacity daily, and 18 trees severely water stressed by

146 withholding irrigation. Once severe water stress (SS) levels were reached in these 18 trees (day

147 0), half ($n = 9$) were sampled: xylem sap and tissues were collected and stored for further

148 molecular and chemical analyses. The remaining half ($n = 9$) were watered (REC) during the

149 morning of the same day (day 0) and allowed to fully recover over the period of seven days.

150 After one week of stress relief (day 7), xylem sap and tissues were collected and stored for

151 molecular and chemical analyses. Control plants *(n = 9)* were sampled throughout the

152 experiment. Physiological parameters (Ψ_{stem}, stomatal conductance and photosynthesis), were

153 monitored throughout the entire experiment (i.e. from the start of the stress treatment until full

154 recovery of physiological functions) in droughted and control trees belonging to the second

155 group. A detailed schematic representation of measurements/sampling timing is provided in

156 Figure 1.

157

158 *Measurements of stem hydraulic conductivity*

159 Stem hydraulic conductivity was measured using a standard approach described previously by

160 the authors (Secchi & Zwieniecki, 2012). In short, a long stem was cut under water and this

161 initial cut was followed within a few minutes by cutting a set of three stem segments, each

162 measuring approximately 4 cm. Segments were excised under water approximately 20–30 cm

163 from the initial cut (a distance longer than 2 times the length of vessels in studied poplar). The

164 initial hydraulic conductance (ki) of each stem segment was measured gravimetrically by

165 determination of the flow rate of filtered 10 mm KCl solution. A water source was located on a

166   balance (Sartorius $\pm$ 0.1 mg) and connected to the stem by a plastic tube. The stem was

167   submerged in a water bath at a level approximately 10 cm below the water-level on the balance.

168   After a steady flow rate was reached (a few minutes), the tube connecting the stem to the balance

169   was closed, and a bypass was used to push water across the segment under approximately 2 bars

170   of pressure for approximately 20 seconds to remove embolism. Stem conductance was then re-

171   measured to find maximum conductance (kmax). The PLC was calculated as PLC = 100 * (kmax

172   - ki)/ kmax.

173

174   *Measurements of stem water potential and leaf gas exchange*

175   For each plant, Ψ_{stem} was measured on equilibrated non-transpiring (bagged) leaves. First, mature

176   leaves were covered with aluminum foil and placed in a humidified plastic bag for at least 30

177   minutes before excision. After excision, leaves were allowed to equilibrate for more than 20

178   minutes in dark conditions before being measured for water potential with a Scholander-type

179   pressure chamber (Soil Moisture Equipment Corp., Santa Barbara, CA, USA). Physiological

180   parameters were monitored daily (between 9:00 AM and 12:00 PM) for the duration of the

181   experiments.

182   Stomatal conductance (g_s) and net photosynthesis (A_N) were measured on fully expanded leaves

183   exposed to direct sunlight, using a portable infrared gas analyzer (ADC-LCPro+ system, The

184   Analytical Development Company Ltd, Hoddesdon, UK). Measurements were performed using a

185   6.25 cm^2 leaf chamber equipped with artificial irradiation (1200 µmol photon m^{-2} s^{-1}), set with a

186   chamber temperature of 25°C to avoid leaf overheating. CO_2 values were maintained at

187   greenhouse conditions (400-450 ppm) for the duration of experimental trial.

188

189 *Sap and stem sampling procedure*

190 Xylem sap from functional vessels was collected from treated (SS-day 0 and REC-day 7, Fig. 1)

191 and CTR plants, according to a previously described method (Secchi & Zwieniecki, 2012). Sap

192 samples were kept at -20°C until analyses of ABA content, pH and soluble carbohydrate content

193 were conducted. Using the same poplar stems taken for sap collection, wood samples were

194 collected by peeling the bark and scraping the xylem using a sterile blade. Once collected, wood

195 samples were immediately frozen in liquid nitrogen and kept at -80°C for further analysis (gene

196 expression, starch and glucose content and enzymatic activity).

197

198 *HPLC-MS/MS analysis of sap abscisic acid (ABA) content*

199 ABA concentration was quantified following the method described by Siciliano *et al.* (2015),

200 with minor modifications. After thawing, 50-100 µL of each biological replicate was centrifuged

201 at 13000 g and 4 °C for 5 minutes. The obtained supernatant was filtered through a 0.2 µm

202 syringe filter and collected in a 1 mL amber glass vial containing a glass insert (Supelco, Sigma-

203 Aldrich) for small sample volumes and analyzed by HPLC-MS/MS. High Performance Liquid

204 Chromatography was carried out using a 1260 Agilent Technologies (Waldbronn, Germany)

205 system equipped with a binary pump and a vacuum degasser. Sample aliquots (20 µL) were

206 injected on a Luna C18 (150 × 2 mm i.d., 3 µm Phenomenex, Torrance, CA), ABA was eluted in

207 isocratic conditions of 65:35 (H_2O:CH_3CN v/v acidified with HCOOH 0.1%) under a flow of

208 200 µL min^{-1} for 5 minutes. Using an electrospray (ESI) ion source operating in negative ion

209 mode samples were introduced into a triple-quadruple mass spectrometer (Varian 310-MS TQ

210 Mass Spectrometer). Analyses were conducted in MRM mode using two transitions: 263>153

211 (CE 12V) for quantification, 263>219 (CE 12V) for monitoring, with 2 mbar of Argon (Ar) as

212   the collision gas. The external standard method was applied to quantify ABA concentration in

213   target samples. A standard curve was generated using an original ABA standard (Sigma Aldrich,

214   St Louis, MO, USA; purity 98.5 %), with concentrations ranging from 10 to 500 µg L^{-1}.

215   Detection (LOD) and quantification (LOQ) limits were calculated based on the standard

216   deviation of the response (σ) and slope of the calibration curve (S) ratio in accordance with the

217   ICH Harmonized Tripartite Guideline expressed as: LOD=3.3σ/S; LOQ=10σ/S. Calculated final

218   values were as follows: LOD = 0.87 ng mL^{-1}; LOQ = 2.90 ng mL^{-1}.

219

220   *Analysis of starch and glucose concentrations in wood samples*

221   Frozen wood samples were ground to a fine powder using a tissue lyser system (TissueLyser II,

222   Qiagen), and starch content was quantified by enzymatic assay (STA-20 kit; Sigma-Aldrich), as

223   detailed by (Secchi & Zwieniecki, 2011). Starch content was represented by the amount of

224   released glucose, which was determined by colorimetric reaction using a glucose oxidase-

225   mediated method in accordance with the manufacturer's instructions. Sample absorbance was

226   read at 540 nm, and starch concentrations were calculated using the glucose standard curve as a

227   reference and expressed as mg g^{-1} of fresh wood. Wood starch amounts were determined for all

228   plants considered in the experiment.

229   For glucose measurements, 15 ± 1 mg sample of the same material was transferred into a 1.5 mL

230   test tube. Each wood sample received 0.3 mL of 80 % ethanol solution before incubating twice at

231   80°C for 30 minutes. A third incubation was performed in 0.5 mL of assay buffer solution (50

232   mM Tris-HCl, pH 7.5). Glucose content was measured using the method described for sap.

233

234   *In vitro enzymatic assays*

235   For starch analysis, 50 µg of each sample were ground to a fine powder and suspended in 500 µL

236   of acetate buffer. Samples were carefully mixed and centrifuged at 15000 rpm (Model 5415 C,

237   Eppendorf, Milan, Italy) and the resulting supernatant was used to establish the basal

238   concentration of glucose (the enzymatic method described above). Samples were then incubated

239   at 55°C and 1 mM maltose was added to each. The glucose released by the hydrolysis of maltose

240   due to native wood amiloglucosidases was measured after 5, 10, 30, 60 and 90 minutes, in order

241   to define the linearity (inflexion point approx. at 60 minutes). *In vitro* amiloglucosidase activity

242   was evaluated by subtracting the basal concentration of glucose from the glucose value measured

243   after 30 minutes. Amiloglucosidase activity was expressed as hydrolyzed maltose (μmol min^{-1} g^{-1}

244   ^{1} FW).

245

246   *Measurements of pH and soluble carbohydrates in xylem sap*

247   The pH measurements were taken on sap samples collected from CTR, SS and REC poplars

248   using a micro pH electrode (PerpHect® ROSS®, Thermo Fischer Scientific, Waltham, MA

249   USA). Concentrations of non-structural carbohydrates (NSC) in xylem sap were quantified

250   following the anthrone-sulfuric acid assay described by (Leyva *et al.*, 2008); in short 50 µl of

251   xylem sap were added to 150 µl of fresh anthrone reagent [0.1 g of anthrone (0.1%) in 100 mL of

252   concentrated sulfuric acid (98%)], samples were mixed, kept for 10 minutes at 4 °C and then

253   incubated for 20 minutes at 100 °C. After heating, samples were cooled for 20 minutes at room

254   temperature before absorbance was read at 620 nm with a microplate reader (iMark Microplate

255   Absorbance Reader, Bio-Rad). A glucose standard curve was used to compare the colorimetric

256   response of the samples, and the NSC content was expressed as moL L^{-1} of glucose.

257 For glucose measurements, 5-20 µL of sap were transferred to a cuvette with 2 mL (final

258 volume) of assay buffer solution (50 mM Tris-HCl, pH 7.5, with 5 mM $MgCl_2$, 125 µM $NADP^+$,

259 and 1 mM MgATP at 37°C) and placed in a spectrofluorimeter (LS50B Luminescence

260 Spectrometer, Perkin-Elmer, MA, USA). The reaction was conducted by adding 2U of both

261 glucose-6-phosphate dehydrogenase and hexokinase. When enzymatic kinetics reached a steady

262 state, fructose was evaluated by adding 3U of phosphoglucose isomerase to convert hexokinase-

263 produced fructose-6-phospate to glucose-6-phospate. Glucose concentration was then estimated

264 from a calibration curve of known glucose amounts.

265 For sucrose analysis, 10-20 µL of the supernatant were placed in a 1.5 mL test tube with 400 µL

266 of acetate buffer and 20 U of invertase enzyme to break down sucrose into fructose and glucose.

267 Test tubes were then incubated at 55°C in a water bath for 30 minutes. The same procedure was

268 followed for the digestion of starch breakdown soluble sugars (SSBP; maltose and its isoforms:

269 isomaltose and maltodextrins), using 25 U of α-amyloglucosidase per sample. To prevent further

270 degradation, sap samples were boiled for 3 minutes. For the spectrofluorimetric analysis of the

271 glucose produced by these reactions, 10-20 µL of supernatant were transferred into a cuvette

272 with 2 mL (final volume) of assay buffer following the same glucose quantification procedure

273 described above. Finally, to quantify the amount of sucrose and SSBP, the baseline quantity of

274 glucose was subtracted from quantities measured after the invertase and α-amyloglucosidase

275 reactions. All chemicals and enzymes used were from Sigma Aldrich (St Louis, MO, USA).

276 In addition, we compared NSC quantities in xylem sap using the anthrone-sulfuric acid assay in

277 parallel with the enzymatic method (see above). A correlation between the two procedures (Fig.

278 S1), confirmed the reliability of both techniques.

279

280   *Real Time PCR experiments on wood samples*

281   Expression changes of target transcripts were analyzed on wood samples collected from control

282   CTR, SS, and REC poplars by quantitative real-time PCR (RT-qPCR). Frozen wood samples

283   were first ground in sterile mortars using liquid nitrogen and further powdered by means of a

284   tissue lyser system (TissueLyser II, Qiagen). Total RNA was extracted from 200 mg of

285   powdered tissue following the method described by (Chang *et al.*, 1993) with slight

286   modifications. Total RNA yield and purity were checked by spectrophotometry (Nanodrop ND-

287   1000; Thermo Fisher Scientific), whereas RNA sample integrity was assessed by electrophoresis

288   gel analysis. In order to avoid any risk of genomic DNA contamination, RNA samples were

289   treated with DNase I (Invitrogen; Thermo Fisher Scientific) in accordance with the

290   manufacturer's instructions. For each biological replicate, first-strand cDNA was synthesized

291   from 1 μg of total RNA using the High Capacity cDNA Reverse Transcription Kit (Applied

292   Biosystems; Thermo Fisher Scientific), following the manufacturer's instructions. Real Time

293   PCR reactions were carried out in a StepOnePlus^{TM} RT-qPCR System (Applied Biosystems;

294   Thermo Fisher Scientific), using the SYBR Green (Applied Biosystems; Thermo Fisher

295   Scientific) method for quantifying amplification results. Thermal cycling conditions were as

296   follows: an initial denaturation phase at 95°C for 10 minutes, followed by 45 cycles at 95°C for

297   15 seconds and 60°C for 1 minute. Expression levels of target transcripts were quantified after

298   normalization to *Ubiquitin* (*PtUBI*) and *Actin* (*PtACT*) genes, both served as internal controls.

299   Gene-specific primers used in Real Time PCR experiments are listed in Table S1. Real time PCR

300   assays were carried out using three biological replicates per treatment-type and three technical

301   replicates were run for each of the three biological replicates.

302

Statistical analyses

304   Significant differences among treatments were statistically analyzed by applying a one-way

305   analysis of variance (ANOVA). Tukey's *HSD* post-hoc test was used for separating means when

306   ANOVA results were significant (*P < 0.05*). Significant differences between pairwise

307   comparisons were assessed by applying Student's *t*-test. The SPSS statistical software package

308   (v24.0, SPSS Inc., Cary, NC, USA) was used to run the statistical analyses, and Sigma Plot

309   software (Systat Software Inc., San Jose, USA) was used to create figures.

310

311   **Results**

312   Potted poplar trees reached a severe water stress level of -2.4 MPa (average stem water potential;

313   Ψ_{stem}) after 11 days of imposed drought treatment (Fig. 2, day 0). The high level of drought

314   imposed caused a severe loss of hydraulic conductivity (80% ± 9.4 of PLC, Fig. 3); and although

315   the leaves lost their turgor, they did not shed, as shown in Fig. 3. Three days prior to a significant

316   drop in stem water potential, stomatal conductance (g_s) and photosynthetic rate (A_N) were

317   significantly lower in plants exposed to drought than in control trees (Fig. 2). At severe water

318   stress levels stomata were fully closed (Fig. 2B; day 0). Half of the stressed plants (9 in total)

319   were watered during the morning of day 0 and within several hours (day 1) Ψ_{stem} recovered close

320   to control-plant levels (Fig. 2C). However, both g_s and A_N remained significantly lower and did

321   not recover to pre-stress conditions until after three days of stress relief (Fig. 2A, B; day 3).

322   Moreover, one day after stress relief, poplars did not recover from embolism formation (PLC=

323   64.2 ± 22.7), while a significant drop in the level of PLC, comparable to pre-stress level, was

324   measured within seven days of watering (Fig. 3). Xylem sap ABA contents were significantly

325   higher (up to 100 fold) in stressed plants (day 0) compared to control plants (Table 1). However,

326 after one week of rehydration ABA decreased to pre-stress values, reaching levels similar to

327 those measured in control trees (12.57 $\pm$ 5.49 µg L^{-1} and 12.41 $\pm$ 1.65 µg L^{-1}, respectively),

328 (Table 1).

329   Drought stress coincided with significant xylem sap acidification, from a pH of 6.28 $\pm$

330 0.037 in control plants to 5.94 $\pm$ 0.042 in stressed plants (Table 1, Fig. 4A). Relief from water

331 stress did not result in a pH recovery to pre-stress conditions even after seven days (Table 1, Fig.

332 4A). Under drought conditions, the acidification of xylem sap occurred in parallel with a

333 significant increase in apoplastic soluble carbohydrate content (Fig. 4B). In SS poplars, NSC

334 concentrations in xylem sap reached average values of 7.08 e^{-03} $\pm$ 1.31 e^{-03} mol L^{-1} (equivalent to

335 0.2 bar, a similar level as previously found in functional vessels of stressed poplar plants; Secchi

336 & Zwieniecki, 2012), up to four times higher than in CTR plants (Table 2). The total amount of

337 carbohydrates in the sap returned to pre-stress levels when water-stress was alleviated, with

338 values overlapping those of irrigated poplars (Fig. 4B).

339   Plants subjected to water stress also exhibited a lower starch concentration in wood

340 samples (1.7 $\pm$ 0.10 mg g^{-1} FW) compared to CTR poplars (13.2 $\pm$ 0.47 mg g^{-1} FW) (Table 3).

341 The drop in concentration coincided with a transcriptional increase of beta-amylase-encoding

342 genes (Fig. 5A). Drought stress was associated with an increase of transcript levels of *PtBMY1a,*

343 *PtBMY1b* and to a lesser extent of *PtBMY3*. However, among the studied genes, only *PtBMY1a*

344 was significantly over-expressed in the presence of stress. Interestingly, *PtBMY5* was the only

345 gene over-expressed exclusively upon re-hydration and not under drought conditions (Fig. 5A).

346 Since the final product of starch hydrolysis is maltose and its isoforms, the content of these

347 products was quantified in the sap of SS poplars and was found to be five times higher than that

348 measured in CTR sap (Table 2). Analysis of expression of a gene encoding a maltose transporter,

349 homologous to *AtMEX1*, also revealed an up-regulation in SS samples, which paralleled the

350 increase in levels of sap maltose isoforms (Fig. 5B and Table 2). Since maltose derived from

351 starch hydrolysis is further metabolized into glucose (Lu & Sharkey, 2006), we assessed both

352 maltase (amyloglucosidase) activity and glucose content in woody tissues. We observed that

353 maltase enzymatic activity had a tendency to increase in stressed tissues (Fig. 6), in agreement

354 with the higher abundance of glucose found in SS wood samples (Table 3). In parallel to higher

355 levels of maltose transporter transcripts, we found significant up-regulation of *PtSUT4*, a gene

356 encoding a cellular membrane sucrose transporter (Fig. 5C). Transcriptional analysis, performed

357 on wood samples, showed that *PtSUT4* was exclusively up-regulated in SS plants (Fig. 5C).

358 　　　Analysis of basic sugar composition showed that sucrose concentrations in xylem sap

359 slightly increased when water stress was induced, although not significantly, starting from $3.42\ \mathrm{e}^{-04} \pm 4.37\ \mathrm{e}^{-05}\ \mathrm{mol\ L}^{-1}$

360 $^{04} \pm 4.37\ \mathrm{e}^{-05}\ \mathrm{mol\ L}^{-1}$ and reaching values of $5.11\ \mathrm{e}^{-04} \pm 1.35\ \mathrm{e}^{-04}\ \mathrm{mol\ L}^{-1}$ when Ψ_{stem} was below -2

361 MPa (Table 3). In contrast, drought strongly increased glucose and fructose amounts in xylem

362 sap, making them most abundant sugars in the apoplast of SS poplars, with up to 10 times the

363 concentrations measured in CTR and REC samples (Table 3). Increased monosaccharide content

364 was associated with higher levels of invertase expression; *PtCWINV1*, *PtCWINV2*, and

365 *PtCWINV4* were previously found to be stem specific (Chen *et al.*, 2015). The *PtCWINV1* and

366 *PtCWINV2* genes were expressed about ten and twenty times more than *PtCWINV4*, respectively

367 and both were significantly up-regulated during stress and recovery. *PtCWINV4* transcription

368 was exclusively induced in severely stressed samples characterized by an acidic apoplastic

369 environment (Fig. 5D).

370

371 **Discussion**

17

372 *Dynamics of physiological responses to severe drought followed by watering*

373 Trees responded to increasing water stress with gradual decreases in net assimilation rate and

374 stomatal conductance. More severe stress (ψ_{stem}< -2 MPa) strongly impacted e xylem hydraulic

375 conductance inducing high levels of embolism formation (80% PLC), indicative of vulnerability

376 to drought-induced cavitation in *P. tremula x alba* (Secchi & Zwieniecki, 2014). Although

377 rehydration caused a fast recovery of stem water potential to pre-stress conditions, both A_N, g_s

378 took three to seven days to fully recover, most likely the time needed to fully restore the stem's

379 hydraulic capacity. This pattern of delayed recovery in stomatal conductance and photosynthetic

380 processes, despite a quick recovery in xylem pressure, is consistent with previous results

381 obtained in poplar (Secchi & Zwieniecki, 2014) and other woody plants, such as eucalyptus

382 (Martorell *et al.*, 2014), grapevine (Chitarra *et al.*, 2014, Lovisolo *et al.*, 2008, Mitchell *et al.*,

383 2013), laurel (Trifilo *et al.*, 2017) and conifers (Brodribb & McAdam, 2013). Potted poplar trees

384 grown in similar conditions were able to recover from embolism formation after water relief and

385 under low or moderate tension; thus the results presented here are consistent with data of xylem

386 hydraulic recovery measured respectively in *Populus trichocarpa* (Secchi & Zwieniecki, 2011),

387 *P. nigra* (Secchi & Zwieniecki, 2012), and in the same clone used here (*Populus alba x tremula*;

388 Secchi & Zwieniecki, 2014).

389 Besides hydraulic factors, delayed stomatal opening could be attributed to non-hydraulic

390 chemical signals, such as abscisic acid (ABA) levels or xylem sap chemistry (Lovisolo *et al.*,

391 2002, Pantin *et al.*, 2013, Schachtman & Goodger, 2008). In this study, the decrease of xylem

392 ABA sap content to pre-stress levels, which occurred over the period of seven days, coincided

393 with the increase in stomatal opening. We can consider the observed delay in g_s recovery as a

394 time buffer between the restoration of water potential and the onset of transpiration (Secchi &

395 Zwieniecki, 2014). In perennial plants, this buffer may provide the necessary time to repair the

396 hydraulic transport capacity lost to embolism. Collectively, these results point to a dynamic

397 regulation of stomatal and g_s recovery processes that may be influenced by a complex network of

398 factors (i.e. changes in endogenous abscisic acid levels and/or efficiency of the photosynthetic

399 system) beyond water supply through the xylem and stem water pressure.

400

401 *Metabolism and partitioning between starch and soluble carbohydrates during drought and*

402 *recovery*

403 The ability of trees to repair xylem functionality after a short-term drought treatment is highly

404 correlated with carbohydrate content in the stem (Trifilò *et al.*, 2017). Starch metabolism is

405 considered to be at the forefront of plant response to embolism formation. Several studies have

406 demonstrated that the presence of embolisms alters the metabolism and partitioning of starch and

407 soluble carbohydrates, as well as their associated enzymatic activities and gene expression

408 (Regier *et al.*, 2009, Salleo *et al.*, 2004, Secchi & Zwieniecki, 2011). Under stress conditions,

409 both glucose content and maltase activity increased in stem parenchyma cells, thus confirming

410 starch degradation as one of the initial plant responses to drought. The reduction in the starch

411 content of stressed plants that we observed, is probably dependent on an enhanced degradation

412 rate (Lu & Sharkey, 2006, Niittyla *et al.*, 2004, Weise *et al.*, 2005). Indeed, in SS samples

413 MEX1, a maltose transporter-encoding gene homologous to *MEX1* in Arabidopsis known to

414 direct maltose efflux to the cytoplasm (Niittyla *et al.*, 2004), was up-regulated. Up-regulation of

415 MEX1, along with the concurrent increases in glucose content in parenchyma cells and maltose

416 isoform levels in xylem sap, further supports the starch degradation process. Considering that,

417 besides MEX, membrane SUT transporters also participate in the transport of maltose (Scofield

418   *et al.*, 2007), while their gene expression is up-regulated under stress in poplar (Secchi *et al.*,

419   2011, Secchi & Zwieniecki, 2011), the increased cytoplasmic concentration of maltose isoforms

420   may have led to efflux via SUT transporters and ultimately to the increase of maltose isoforms in

421   xylem sap.

422   Moreover, analysis of beta-amylase expression, a crucial component for initiating the

423   starch degradation process (Lu & Sharkey, 2006), further reinforces the idea that water stress

424   triggers starch degradation. During the day, and/or when dehydration or osmotic stress occurs,

425   BMY1 is the primary enzyme involved in starch breakdown (Valerio *et al.*, 2011, Zanella *et al.*,

426   2016). Here, *BMY1a* expression was up-regulated in SS wood samples, similarly, *BMY1a* was

427   the only up-regulated *β-amylase* gene in the wood of *P. trichocarpa* under different osmotic

428   stress treatments (Secchi & Zwieniecki, 2011). Interestingly, among the analyzed amylase genes,

429   *BMY5* was over-expressed only upon rehydration. Although a clear understanding of the

430   functional role of BMY5 is still missing, its up-regulation in REC samples, combined with a

431   reduced starch content, is consistent with the over-expression of its homologous gene in

432   *Arabidopsis* starch-less mutants (Monroe & Preiss, 1990), suggesting a potential involvement of

433   BMY5 in the regulation of starch turnover during stress recovery.

434   Under drought stress, sugars in the xylem apoplast can accumulate either from the stored

435   products of starch degradation in parenchyma cells (maltose and sucrose) or translocation from

436   phloem to parenchyma rays (sucrose). Apoplastic accumulation can be either passive i.e. leaking

437   of sugars across membranes due to large concentration differences between the apoplast and

438   living cells, actively facilitated by membrane sugar transporters. The sucrose transporter *SUT4*, a

439   protein homologous to the maize *SUT1*, is a phloem-localized bidirectional symporter which

440   catalyzes both sucrose and proton transport depending on sucrose and pH gradients as well as

441 membrane potential (Carpaneto *et al.*, 2005, Carpaneto *et al.*, 2010). The role of *SUT4* in

442 controlling sucrose transport and partitioning was explored in poplar and it was demonstrated

443 that at the stem level, in addition to phloem cells, SUT4 is also expressed in ray parenchyma

444 cells, fibers and secondary xylem vessels (Payyavula *et al.*, 2011). We found that *SUT4*

445 transcripts were more abundant in SS woody tissues. Therefore, the increased activity of this

446 symporter can facilitate the efflux of both sucrose (and possibly maltose) and protons towards

447 the apoplast, further evidenced by the increase in the total carbohydrate content of sap and by the

448 observed acidification of apoplastic pH. A lower pH and an accumulation of disaccharides can

449 halt the efflux of sugar via SUT transporters to the apoplast and consequently hinder the capacity

450 to build sufficient levels of osmotica for refilling upon stress relief. However, a lower pH can

451 also trigger the activity of apoplastic invertases, reducing the concentration of sucrose, thus

452 maintaining the gradient prompting sucrose efflux.

453

454 *Functional link between drought-induced acidification of xylem sap pH and sugar accumulation*

455 *in the xylem apoplast*

456 Alteration of sap pH is one of the first chemical changes that occurs within the xylem vessels of

457 water stressed plants (Bahrun *et al.*, 2002, Sobeih *et al.*, 2004). Unlike herbaceous plants,

458 drought-induced alkalization of apoplastic pH is not common in trees. Xylem sap acidification

459 has been documented in a number of woody species (Sharp & Davies, 2009), most recently

460 during the summer period in conifers at the alpine timberline (Losso *et al.*, 2017). Here, we show

461 that: i) poplars exposed to severe water stress respond through acidification of the xylem

462 apoplast; ii) a drop of pH under drought is accompanied by the accumulation of soluble

463 carbohydrates; iii) glucose and fructose are the most abundant sugars in sap collected from

464 stressed poplars; iv) starch hydrolysis increases the content of soluble carbohydrates (i.e. maltose

465 is also present in the sap). It was previously proposed that an acidic environment might cause the

466 accumulation of monosaccharides in the xylem apoplast via sucrose hydrolysis mediated by

467 acidic invertases (Secchi & Zwieniecki, 2016). Here, we further support that hypothesis through

468 a gene expression analysis of members of the cell wall acidic invertases (CWINV). We profiled

469 the expression of three genes, *CWINV1*, *CWINV2* and *CWINV4,* among the five members of the

470 recently identified CWINV family in poplar (Chen *et al.*, 2015). *CWINV1*, *CWINV2* and

471 *CWINV4* have been confirmed, by RNA-seq analyses on different tissues, to be expressed in the

472 stem (Chen *et al.*, 2015). The results attest that all three genes were over-expressed during

473 drought, accordingly elevated levels of glucose and fructose accumulated in the sap. Moreover,

474 *CWINV 1* and *2* transcripts were overall more abundant than *CWINV4* (about ten times more for

475 *CWINV1* and almost twenty times more for *CWINV2*), especially during recovery. This strongly

476 implies that the biological control of physiological activity in response to stress is linked to an

477 accumulation of monosaccharides in the xylem. This accumulation, in parallel with the reduction

478 of disaccharide content, results in the steady efflux of disaccharides towards the apoplast − a

479 transport sustained by low apoplastic sucrose concentrations and the fast buildup of

480 monosaccharide osmotica. The fact that pH did not return to the pre-stress conditions within a

481 few days, might reflect a lingering effect of stress or 'memory of stress' that would facilitate

482 future responses in the case of consecutive droughts. Previous observations conducted *in vivo* in

483 poplar stems, a drop in xylem apoplastic pH coincides with loss of stem hydraulic conductivity,

484 and recovery of xylem pH induced by watering is delayed in comparison with recovery of stem

485 water potential (Secchi & Zwieniecki, 2012).

486

Conclusion

In the present study, we strengthen and further support a previously proposed scenario wherein dynamic changes occur in the xylem sap at the onset of drought stress and recovery (Secchi & Zwieniecki, 2016). We characterize, from a molecular and biochemical perspective, the functional link between drought-induced xylem sap acidification and sugar accumulation, demonstrating that these synergistic events are crucial for triggering plant responses to water stress, including the eventual restoration of xylem functionality (Fig. 7). We thus unravel a complex network of molecular and biochemical signals activated at the interface between xylem and parenchyma cells during drought and its subsequent relief. Biochemical and molecular activity result in the upregulation of starch degradation processes under stress, followed by an overexpression of sugar symporters, which facilitate the efflux of disaccharides to the apoplast. Meanwhile, sugar symporter activity also mediates the reduction of xylem pH subsequently increasing acidic apoplastic invertases activity and stimulating the accumulation of apoplastic monosaccharides as the main osmoticum. In addition, water stress results in up-regulation of acidic invertase expression, increasing the potential for monosaccharaide accumulation in the apoplast under stress. These coordinated events suggest 'biological' priming of xylem to expedite stress recovery during the rehydration period. Our work highlights the important role of carbohydrate reserve mobilization in sustaining the energetically demanding processes involved in plant stress responses.

514

References

516 Bahrun A., Jensen C.R., Asch F. & Mogensen V.O. (2002) Drought-induced changes in xylem

517   pH, ionic composition, and ABA concentration act as early signals in field-grown maize

518   (Zea mays L.). *Journal of Experimental Botany*, **53**, 251-263.

519 Barigah T.S., Charrier O., Douris M., Bonhomme M., Herbette S., Ameglio T., Fichot R.,

520   Brignolas F. & Cochard H. (2013) Water stress-induced xylem hydraulic failure is a

521   causal factor of tree mortality in beech and poplar. *Annals of Botany*, **112**, 1431-1437.

522 Brodersen C.R. & McElrone A.J. (2013) Maintenance of xylem network transport capacity: a

523   review of embolism repair in vascular plants. *Frontiers in Plant Science*, **4**.

524 Brodersen C.R., McElrone A.J., Choat B., Matthews M.A. & Shackel K.A. (2010) The

525   Dynamics of Embolism Repair in Xylem: In Vivo Visualizations Using High-Resolution

526   Computed Tomography. *Plant Physiology*, **154**, 1088-1095.

527 Brodribb T.J. & Jordan G.J. (2008) Internal coordination between hydraulics and stomatal

528   control in leaves. *Plant Cell and Environment*, **31**, 1557-1564.

529 Brodribb T.J. & McAdam S.A.M. (2013) Abscisic Acid Mediates a Divergence in the Drought

530   Response of Two Conifers. *Plant Physiology*, **162**, 1370-1377.

531 Carpaneto A., Geiger D., Bamberg E., Sauer N., Fromm J. & Hedrich R. (2005) Phloem-

532   localized, proton-coupled sucrose carrier ZmSUT1 mediates sucrose efflux under the

533   control of the sucrose gradient and the proton motive force. *Journal of Biological*

534   *Chemistry*, **280**, 21437-21443.

535   Carpaneto A., Koepsell H., Bamberg E., Hedrich R. & Geiger D. (2010) Sucrose- and H+-

536   Dependent Charge Movements Associated with the Gating of Sucrose Transporter

537   ZmSUT1. *Plos One*, **5**.

538   Chang S., Puryear J. & Cairney J. (1993) A simple and efficient method for isolating RNA from

539   pine tree. *Plant Molecular Biology Report*, **11**, 113-116.

540   Chen Z., Gao K., Su X.X., Rao P. & An X.M. (2015) Genome-Wide Identification of the

541   Invertase Gene Family in Populus. *Plos One*, **10**.

542   Chitarra W., Balestrini R., Vitali M., Pagliarani C., Perrone I., Schubert A. & Lovisolo C. (2014)

543   Gene expression in vessel-associated cells upon xylem embolism repair in *Vitis vinifera*

544   L. petioles. *Planta*, **239**, 887-899.

545   Choat B., Jansen S., Brodribb T.J., Cochard H., Delzon S., Bhaskar R., Bucci S.J., Feild T.S.,

546   Gleason S.M., Hacke U.G., Jacobsen A.L., Lens F., Maherali H., Martinez-Vilalta J.,

547   Mayr S., Mencuccini M., Mitchell P.J., Nardini A., Pittermann J., Pratt R.B., Sperry J.S.,

548   Westoby M., Wright I.J. & Zanne A.E. (2012) Global convergence in the vulnerability of

549   forests to drought. *Nature*, **491**, 752-+.

550   Hacke U.G., Stiller V., Sperry J.S., Pittermann J. & McCulloh K.A. (2001) Cavitation fatigue.

551   Embolism and refilling cycles can weaken the cavitation resistance of xylem. *Plant*

552   *Physiology*, **125**, 779-786.

553   Holbrook N.M., Ahrens E.T., Burns M.J. & Zwieniecki M.A. (2001) In vivo observation of

554   cavitation and embolism repair using magnetic resonance imaging. *Plant Physiology*,

555   **126**, 27-31.

556   Holbrook N.M. & Zwieniecki M.A. (1999) Embolism repair and xylem tension: Do we need a

557   miracle? *Plant Physiology*, **120**, 7-10.

558   Jensen K.H., Berg-Sorensen K., Bruus H., Holbrook N.M., Liesche J., Schulz A., Zwieniecki

559   M.A. & Bohr T. (2016) Sap flow and sugar transport in plants. *Reviews of Modern*

560   *Physics*, **88**.

561   Losso A., Nardini A., Dämon B. & Mayr S. (2017) Xylem sap chemistry: seasonal changes in

562   timberline conifers Pinus cembra, Picea abies, and Larix decidua. *Biologia Plantarum*.

563   Lovisolo C., Hartung W. & Schubert A. (2002) Whole-plant hydraulic conductance and root-to-

564   shoot flow of abscisic acid are independently affected by water stress in grapevines.

565   *Functional Plant Biology*, **29**, 1349-1356.

566   Lovisolo C., Perrone I., Hartung W. & Schubert A. (2008) An abscisic acid-related reduced

567   transpiration promotes gradual embolism repair when grapevines are rehydrated after

568   drought. *New Phytologist*, **180**, 642-651.

569   Lu Y. & Sharkey T.D. (2006) The importance of maltose in transitory starch breakdown. *Plant*

570   *Cell and Environment*, **29**, 353-366.

571   Martorell S., Diaz-Espejo A., Medrano H., Ball M.C. & Choat B. (2014) Rapid hydraulic

572   recovery in Eucalyptus pauciflora after drought: linkages between stem hydraulics and

573   leaf gas exchange. *Plant Cell and Environment*, **37**, 617-626.

574   Mitchell P.J., O'Grady A.P., Tissue D.T., White D.A., Ottenschlaeger M.L. & Pinkard E.A.

575   (2013) Drought response strategies define the relative contributions of hydraulic

576   dysfunction and carbohydrate depletion during tree mortality. *New Phytologist*, **197**, 862-

577   872.

578   Monroe J.D. & Preiss J. (1990) Purification of a beta-amylase that accumulates in arabidopsis-

579   thaliana mutants defective in starch metabolism. *Plant Physiology*, **94**, 1033-1039.

580   Nardini A., Lo Gullo M.A. & Salleo S. (2011) Refilling embolized xylem conduits: Is it a matter

581   of phloem unloading? *Plant Science*, **180**, 604-611.

582   Niittyla T., Messerli G., Trevisan M., Chen J., Smith A.M. & Zeeman S.C. (2004) A previously

583   unknown maltose transporter essential for starch degradation in leaves. *Science*, **303**, 87-

584   89.

585   Pantin F., Monnet F., Jannaud D., Costa J.M., Renaud J., Muller B., Simonneau T. & Genty B.

586   (2013) The dual effect of abscisic acid on stomata. *New Phytologist*, **197**, 65-72.

587   Payyavula R.S., Tay K.H.C., Tsai C.J. & Harding S.A. (2011) The sucrose transporter family in

588   Populus: the importance of a tonoplast PtaSUT4 to biomass and carbon partitioning.

589   *Plant Journal*, **65**, 757-770.

590   Regier N., Streb S., Cocozza C., Schaub M., Cherubini P., Zeeman S.C. & Frey B. (2009)

591   Drought tolerance of two black poplar (Populus nigra L.) clones: contribution of

592   carbohydrates and oxidative stress defence. *Plant Cell and Environment*, **32**, 1724-1736.

593   Salleo S., Lo Gullo M.A., Trifilo' P. & Nardini A. (2004) New evidence for a role of vessel-

594   associated cells and phloem in the rapid xylem refilling of cavitated stems of *Laurus*

595   *nobilis* L. *Plant, Cell and Environment*, **27**, 1065-1076.

596   Salleo S., Trifilo' P., Esposito S., Nardini A. & Lo Gullo M.A. (2009) Starch-to-sugar conversion

597   in wood parenchyma of field-growing *Laurus nobilis* plants: a component of the signal

598   pathway for embolism repair? *Functional Plant Biology*, **36**, 815-825.

599   Savi T., Casolo V., Luglio J., Bertuzzi S., Trifilo P., Lo Gullo M.A. & Nardini A. (2016)

600   Species-specific reversal of stem xylem embolism after a prolonged drought correlates to

601   endpoint concentration of soluble sugars. *Plant Physiology and Biochemistry*, **106**, 198-

602   207.

603 Schachtman D.P. & Goodger J.Q.D. (2008) Chemical root to shoot signaling under drought.

604   *Trends in Plant Science*, **13**, 281-287.

605 Scheenen T.W.J., Vergeldt F.J., Heemskerk A.M. & Van As H. (2007) Intact plant magnetic

606   resonance imaging to study dynamics in long-distance sap flow and flow-conducting

607   surface area. *Plant Physiology*, **144**, 1157-1165.

608 Scofield G.N., Aoki N., Hirose T., Takano M., Jenkins C.L.D. & Furbank R.T. (2007) The role

609   of the sucrose transporter, OsSUT1, in germination and early seedling growth and

610   development of rice plants. *Journal of Experimental Botany*, **58**, 483-495.

611 Secchi F., Gilbert M.E. & Zwieniecki M.A. (2011) Transcriptome response to embolism

612   formation in stems of *Populus trichocarpa* provides insight into signaling and the biology

613   of refilling. *Plant Physiology*, **157**, 1419-1429.

614 Secchi F. & Zwieniecki M.A. (2011) Sensing embolism in xylem vessels: the role of sucrose as a

615   trigger for refilling. *Plant, Cell and Environment*, **34**, 514-524.

616 Secchi F. & Zwieniecki M.A. (2012) Analysis of Xylem Sap from Functional (Nonembolized)

617   and Nonfunctional (Embolized) Vessels of *Populus nigra*: Chemistry of Refilling. *Plant*

618   *Physiology*, **160**, 955-964.

619 Secchi F. & Zwieniecki M.A. (2014) Down-Regulation of Plasma Intrinsic Protein1 Aquaporin

620   in Poplar Trees Is Detrimental to Recovery from Embolism. *Plant Physiology*, **164**, 1789-

621   1799.

622   Secchi F. & Zwieniecki M.A. (2016) Accumulation of sugars in the xylem apoplast observed

623   under water stress conditions is controlled by xylem pH. *Plant Cell and Environment*, **39**,

624   2350-2360.

625   Sharp R.G. & Davies W.J. (2009) Variability among species in the apoplastic pH signalling

626   response to drying soils. *Journal of Experimental Botany*, **60**, 4361-4370.

627   Sobeih W.Y., Dodd I.C., Bacon M.A., Grierson D. & Davies W.J. (2004) Long-distance signals

628   regulating stomatal conductance and leaf growth in tomato (Lycopersicon esculentum)

629   plants subjected to partial root-zone drying. *Journal of Experimental Botany*, **55**, 2353-

630   2363.

631   Sperry J.S., Adler F.R., Campbell G.S. & Comstock J.P. (1998) Limitation of plant water use by

632   rhizosphere and xylem conductance: results from a model. *Plant Cell and Environment*,

633   **21**, 347-359.

634   Spicer R. (2014) Symplasmic networks in secondary vascular tissues: parenchyma distribution

635   and activity supporting long-distance transport. *Journal of Experimental Botany*, **65**,

636   1829-1848.

637   Stiller V. & Sperry J.S. (2002) Cavitation fatigue and its reversal in sunflower (Helianthus

638   annuus L.). *Journal of Experimental Botany*, **53**, 1155-1161.

639   Tomasella M., Haberle K.H., Nardini A., Hesse B., Machlet A. & Matyssek R. (2017) Post-

640   drought hydraulic recovery is accompanied by non-structural carbohydrate depletion in

641   the stem wood of Norway spruce saplings. *Scientific Reports*, **7**.

642   Trifilò P., Casolo V., Raimondo F., Petrussa E., Boscutti F., Lo Gullo M.A. & Nardini A. (2017)

643   Effects of prolonged drought on stem non-structural carbohydrates content and post-

644   drought hydraulic recovery in Laurus nobilis L.: The possible link between carbon

645   starvation and hydraulic failure. *Plant Physiology and Biochemistry*, **120**, 232-241.

646   Tyree M.T. & Ewers F.W. (1991) The hydraulic architecture of trees and other woody-plants.

647   *New Phytologist*, **119**, 345-360.

648   Tyree M.T., Salleo S., Nardini A., Lo Gullo M.A., Mosca R. (1999) Refilling of embolized

649   vessels in young stems of laurel. Do we need a new paradigm? *Plant Physiology*, **120**,

650   11-22.

651   Tyree M.T. & Zimmermann M.H. (2002) *Xylem Structure and the Ascent of Sap*. (2nd ed.).

652   Springer-Verlag, New York.

653   Valerio C., Costa A., Marri L., Issakidis-Bourguet E., Pupillo P., Trost P. & Sparla F. (2011)

654   Thioredoxin-regulated beta-amylase (BAM1) triggers diurnal starch degradation in guard

655   cells, and in mesophyll cells under osmotic stress. *Journal of Experimental Botany*, **62**,

656   545-555.

657   Weise S.E., Kim K.S., Stewart R.P. & Sharkey T.D. (2005) beta-maltose is the metabolically

658   active anomer of maltose during transitory starch degradation. *Plant Physiology*, **137**,

659   756-761.

660   Zanella M., Borghi G.L., Pirone C., Thalmann M., Pazmino D., Costa A., Santelia D., Trost P. &

661   Sparla F. (2016) beta-amylase 1 (BAM1) degrades transitory starch to sustain proline

662   biosynthesis during drought stress. *Journal of Experimental Botany*, **67**, 1819-1826.

663   Zwieniecki M.A. & Holbrook N.M. (2009) Confronting Maxwell's demon: biophysics of xylem

664   embolism repair. *Trends in Plant Science*, **14**, 530-534.

665

666

667 **Table 1**

668 Measurements of abscisic acid (ABA) and pH from xylem sap samples collected from well

669 irrigated (CTR; day 0), severely stressed (SS; day 0) and recovered (REC; day 7) poplars.

670 Average values of stem water potential (Ψstem) were also reported for each condition.

671

	CTR (Ψ_{stem} = -0.44 ± 0.015 b)	**SS** (Ψ_{stem} = -2.06 ± 0.069 a)	**REC** (Ψ_{stem} = -0.36 ± 0.038 b)
ABA (μg L^{-1})	12.41 ± 1.65 b	1189.16 ± 165.96 a	12.57 ± 5.49 b
pH	6.28 ± 0.037 a	5.94 ± 0.042 b	5.91 ± 0.053 b

672 Values are means ± SE (n = 9, each biological replicate represents a different plant). Different lower case letters
673 following SE values indicate significant differences attested by Tukey's *HSD* test (P < 0.05).

674

675

Table 2

Concentrations of total carbohydrates, glucose, fructose, sucrose and starch breakdown soluble sugars (maltose and its isoforms: isomaltose and maltodextrins; SSBP) measured in xylem sap samples collected from well irrigated (CTR), severely stressed (SS,day 0) and recovered (REC, day 7) poplars. Analysis of total carbohydrate concentration was performed by anthrone method, while single sugars were measured by enzymatic assays. Average values of stem water potential (Ψ_{stem}) were also reported for each condition.

	CTR (Ψ_{stem} = -0.44 ± 0.015 b)	**SS** (Ψ_{stem} = -2.06 ± 0.069 a)	**REC** (Ψ_{stem} = -0.36 ± 0.038 b)
Total carbohydrates (mol L^{-1})	1.37 e^{-03}± 1.54 e^{-04} b	7.08 e^{-03}± 1.3 e^{-03} a	1.84 e^{-03}± 8.32 e^{-04} b
Glucose (mol L^{-1})	1.23 e^{-04} ± 1.59 e^{-05} b	1.55 e^{-03} ± 3.96 e^{-04} a	8.78 e^{-05} ± 3.42 e^{-05} b
Fructose (mol L^{-1})	9.14 e^{-05} ± 1.86 e^{-05} b	1.69 e^{-03} ± 3.21 e^{-04} a	7.70 e^{-05} ± 3.85 e^{-05} b
Sucrose (mol L^{-1})	3.42 e^{-04} ± 4.37 e^{-05} a	5.11 e^{-04} ± 1.35 e^{-04} a	1.77 e^{-04} ± 1.19 e^{-05} a
SSBP (mol L^{-1})	1.15 e^{-04} ± 1.11 e^{-05} b	5.05 e^{-04} ± 1.71 e^{-04} a	7.34 e^{-04} ± 0.84 e^{-05} b

Values are means ± SE (n = 9, each biological replicate represents a different plant). Different lower case letters following SE values indicate significant differences attested by Tukey's *HSD* test (P < 0.05).

688 **Table 3**

689 Measurements of starch and glucose content in stem wood samples collected from well irrigated

690 (CTR), severely stressed (SS, day 0) and recovered (REC, day 7) poplars. Average values of

691 stem water potential (Ψ_{stem}) were also reported for each condition.

692

	CTR (Ψ_{stem} = -0.44 ± 0.015 b)	**SS** (Ψ_{stem} = -2.06 ± 0.069 a)	**REC** (Ψ_{stem} = -0.36 ± 0.038 b)
Starch (mg g^{-1} FW)	13.2 ± 0.47 a	1.7 ± 0.10 b	4.0 ± 0.18 b
Glucose (mg g^{-1} FW)	1.57 ± 0.20 a	2.04 ± 0.41 a	0.67 ± 0.26 b

693 Values are means ± SE (n = 9, each biological replicate represents a different plant). Different lower case letters
694 following SE values indicate significant differences attested by Tukey's *HSD* test (P < 0.05).

695

Figure legends

697 **Figure 1**

698 Timing schematic representation of measurements/sampling over the duration of the experiment.

699 Ψ_{stem}, stomatal conductance and photosynthesis were monitored throughout the entire experiment

700 i.e. from the start of the stress treatment (day -11) until full recovery of physiological functions

701 (day 7). PLC was measured on stressed and recovered poplars respectively at day 0, 1 and 7

702 (grey circles), while on control plants trough out the experiment duration (white circles).

703 Chemical and molecular analyses were performed on sap and woody tissues collected at day 0

704 for stressed plants and at 7 days for recovered plants (grey circles). Sap and tissues from control

705 plants were sampled trough out the experiment duration (white circles).

706

707 **Figure 2**

708 Measurements of **(A)** assimilation (A_N, μmol CO_2 m^{-2} s^{-1}), **(B)** stomatal conductance (g_s, mmol

709 H_2O m^{-2} s^{-1}) and **(C)** xylem pressure (Ψ_{stem}, MPa) over the progression of drought stress (SS) and

710 recovery (REC).

711 Black dots indicate average values for each parameter, while grey and blue dots refer to single

712 measurements of each parameter taken on SS and REC plants on each experimental day,

713 respectively. The light blue rectangle represents the average value of each parameter measured

714 on well irrigated (CTR) plants. Day -11 represents the beginning of the water stress treatment;

715 Day 0 coincides with higher level of stress and with the moment of rehydration and Day 7 with

716 full recovery. Asterisks denote significant differences between treated (SS or REC) and irrigated

717 (CTR) plants on each day of measurements, tested using the Student's t test (*P < 0.05*). Bars

718 represent SD (*n = 9*).

719

Figure 3

(A) Extent of embolism represented as percent of loss of conductivity (PLC) in stem of poplars

(B) Xylem pressure measured using balancing pressure method on transpiring leaves (Ψ_{stem},

MPa). White, grey, dark grey and black bars indicate average values measured in CTR, SS and 1

day and 7 days REC plants, respectively. Uppercase letters above bars denote significant

differences ($P < 0.05$), tested using Tukey's *HSD* test. Error bars represent SE. **(C)** Severely

stressed (day -3) and control poplar plants used in the experiment.

727

Figure 4

Changes in xylem sap pH **(A)** and total carbohydrate concentrations **(B)** as a function of

increasing xylem pressure (Ψ_{stem}, MPa) measured in sap samples collected from severely stressed

(SS), recovered (REC) and well irrigated (CTR) poplars.

Black, white and grey dots indicate average values measured in SS, CTR and REC plants,

respectively. Smaller light grey dots refer to single measurements in SS and CTR or REC plants.

Analysis of total carbohydrate concentrations was performed by anthrone method. Upper case

letters above symbols denote significant differences, tested by Tukey's *HSD* test ($P < 0.05$). Bars

represent SD ($n = 9$).

737

Figure 5

Expression changes of candidate genes involved in sugar metabolism and transport. RT-qPCR

profiles refer to genes encoding **(A)** beta amylases (BMY), **(B)** maltose transporter (MEX1), **(C)**

sucrose transporter (SUT4), and **(D)** cell wall acidic invertases (CWINV). Both Ubiquitin

742   (*PtUBI*) and Actin (*PtACT*) genes were used as endogenous controls for the normalization

743   procedure of transcription levels. Uppercase letters above bars denote significant differences (*P*

744   *< 0.05*), tested using Tukey's *HSD* test. Error bars represent SE (n = 3).

745

746   **Figure 6**

747   Measurement of maltase activity expressed as hydrolyzed maltose (μmol min^{-1} g^{-1} FW) in wood

748   samples obtained from well irrigated (CTR), severely stressed (SS) and recovered (REC) poplar

749   stems. No significant differences were detected among treatments by the Tukey's *HSD* test (*P <*

750   *0.05*). Bars represent SE (*n = 9*).

751

752   **Figure 7**

753   Schematic of poplar stem biological responses analyzed in this study to severe water stress that

754   result in priming of the stem for hydraulic recovery upon relief from stress.

755

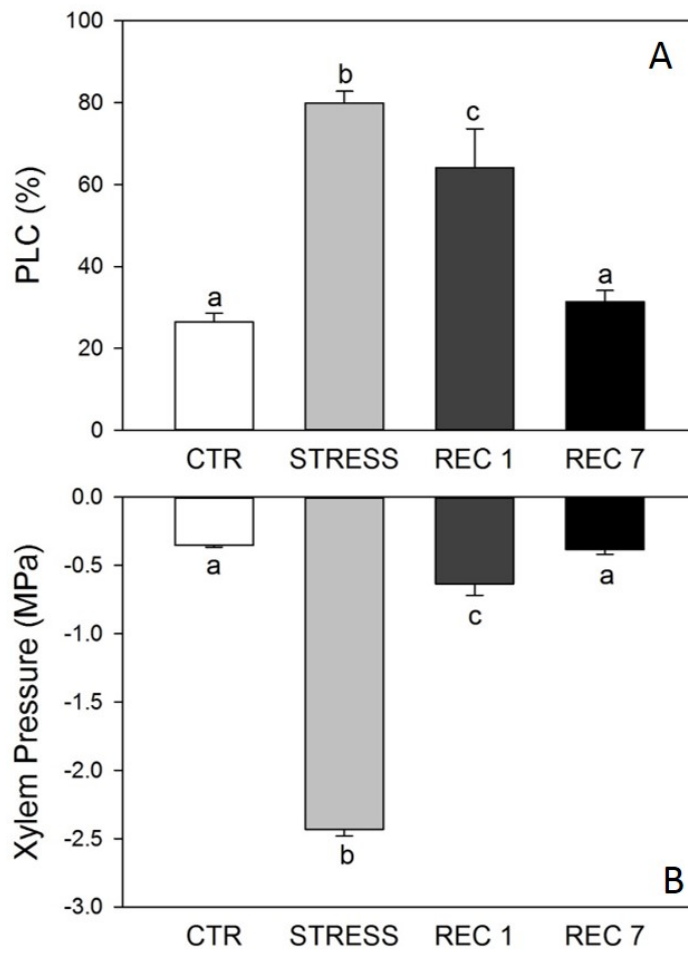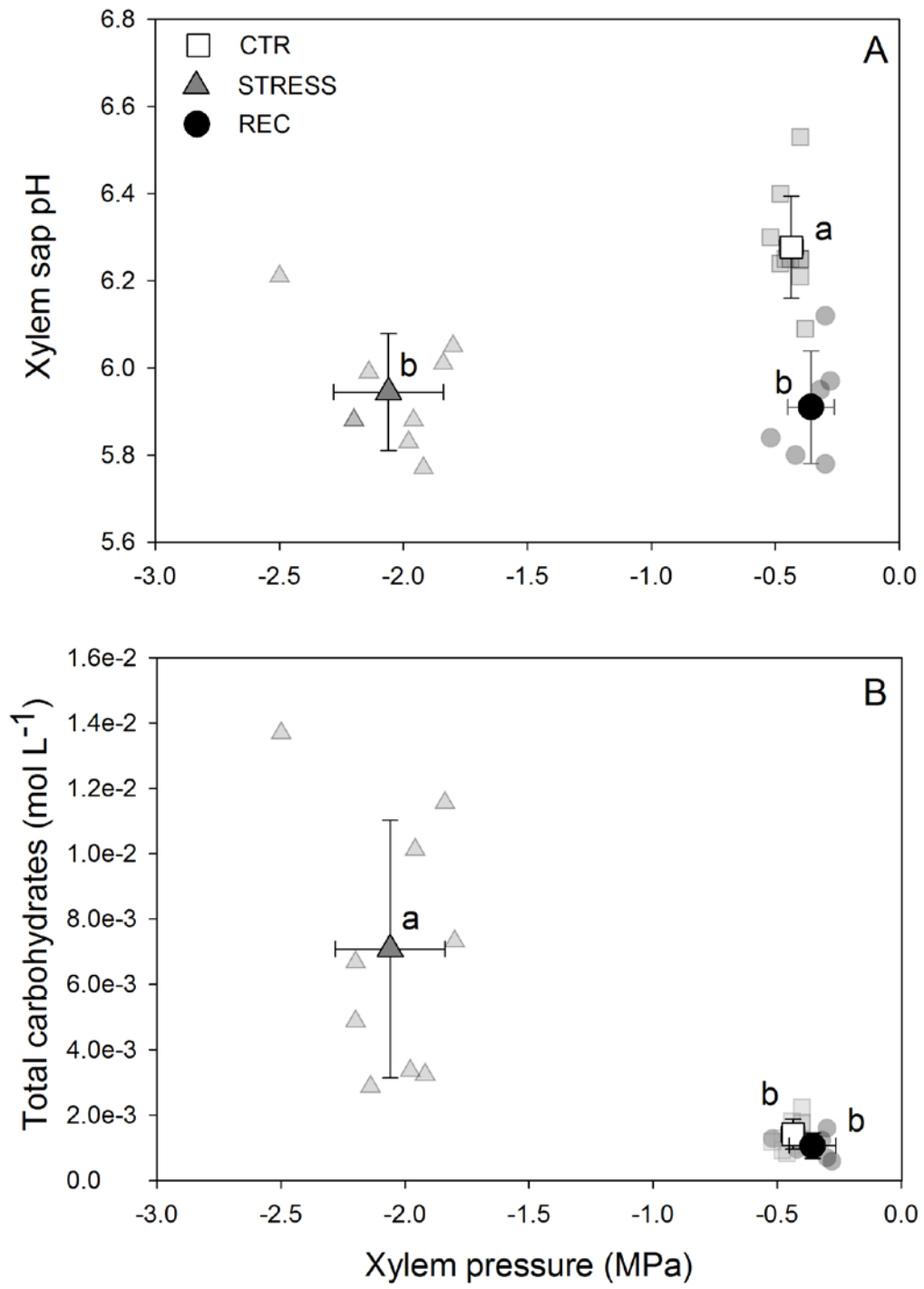756 **Figure 1**

757
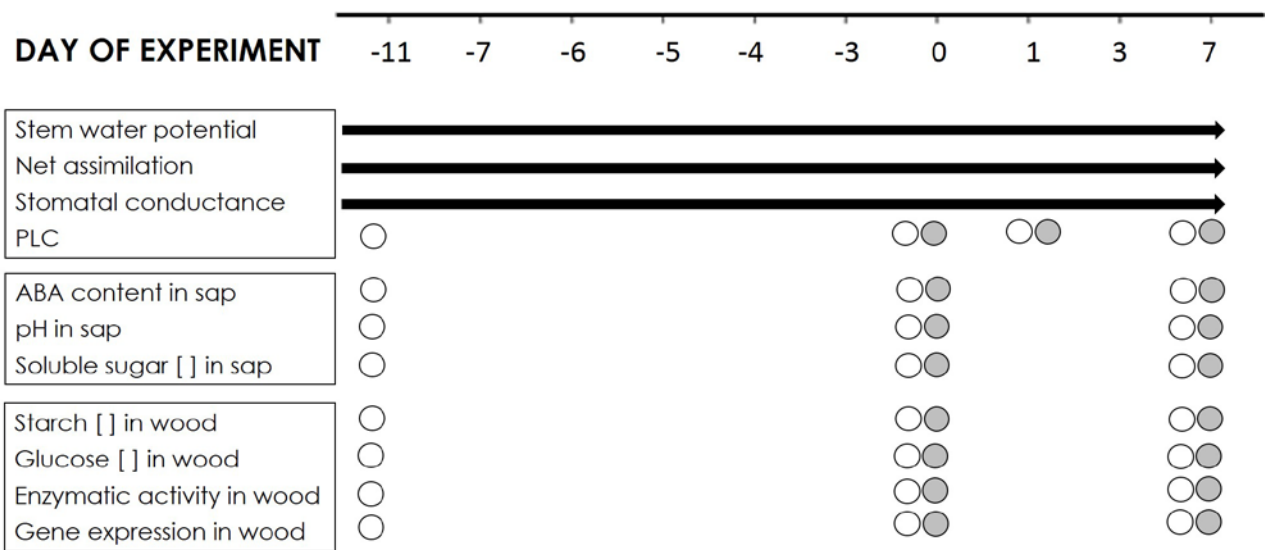
758

759
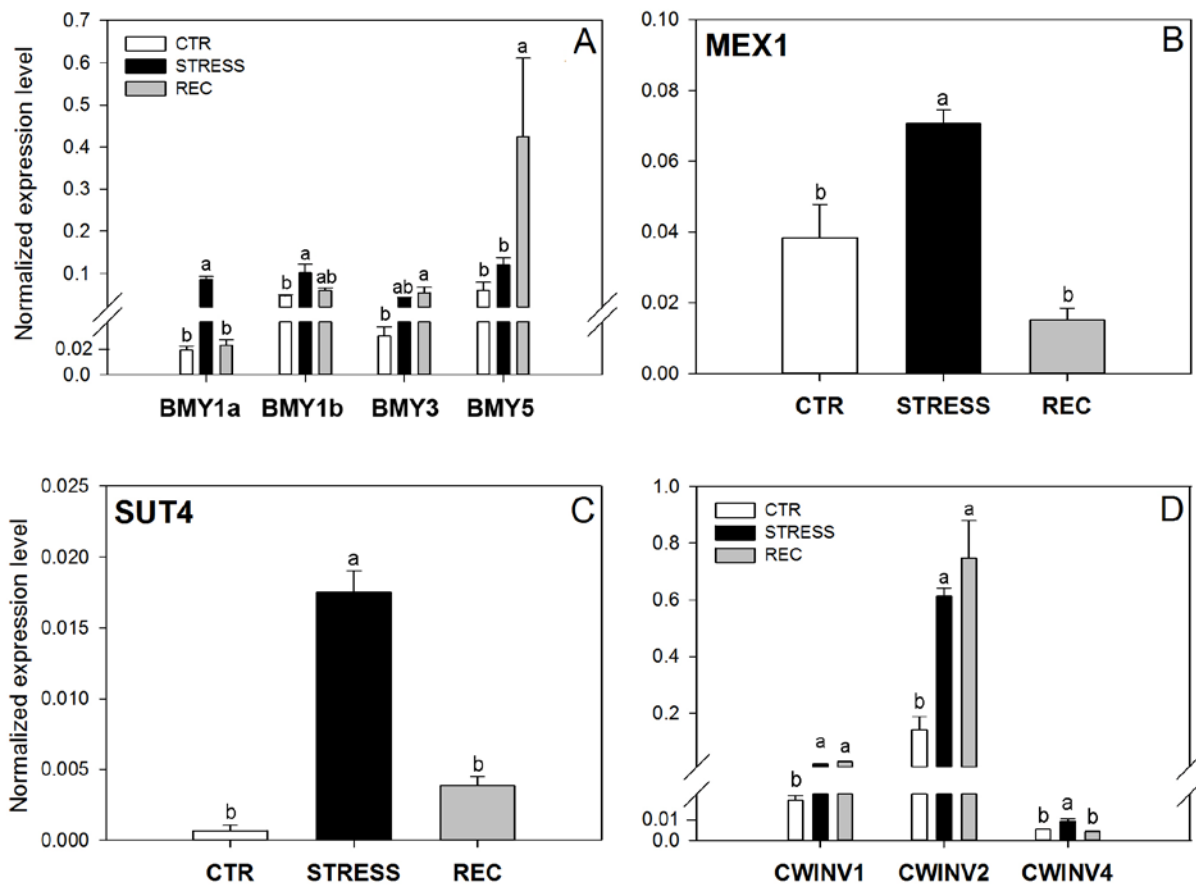
Figure 2

Figure 3
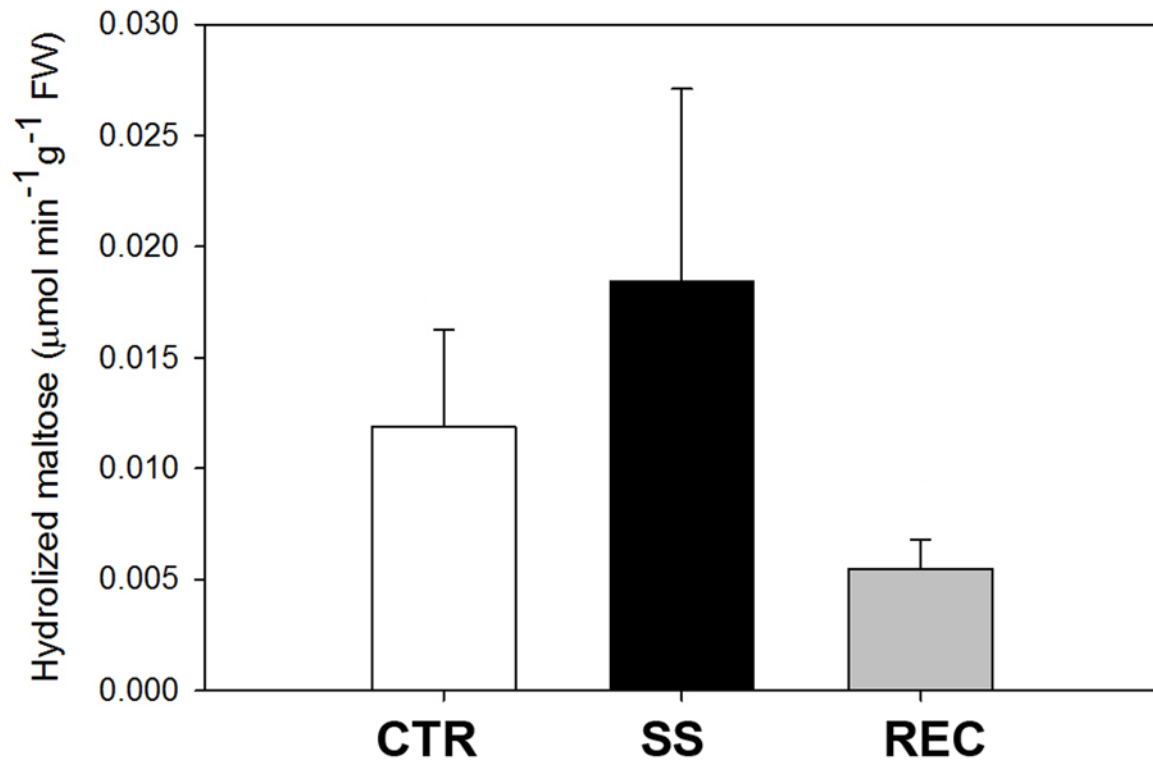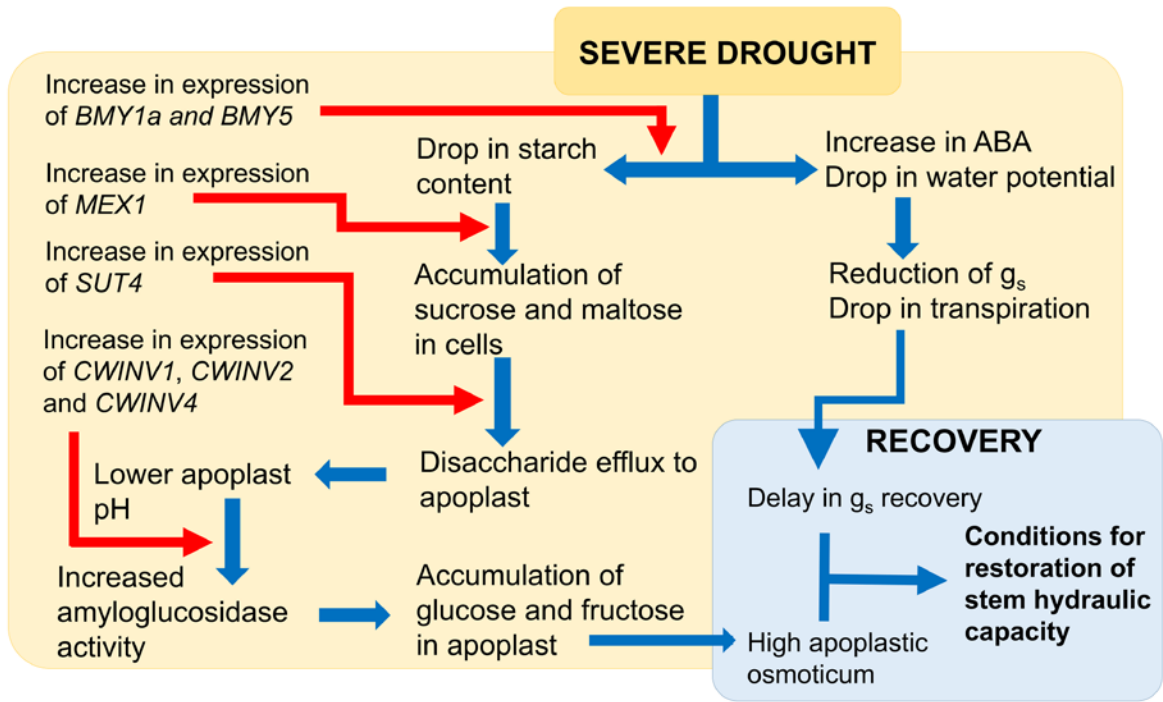
766

Figure 4

768

769
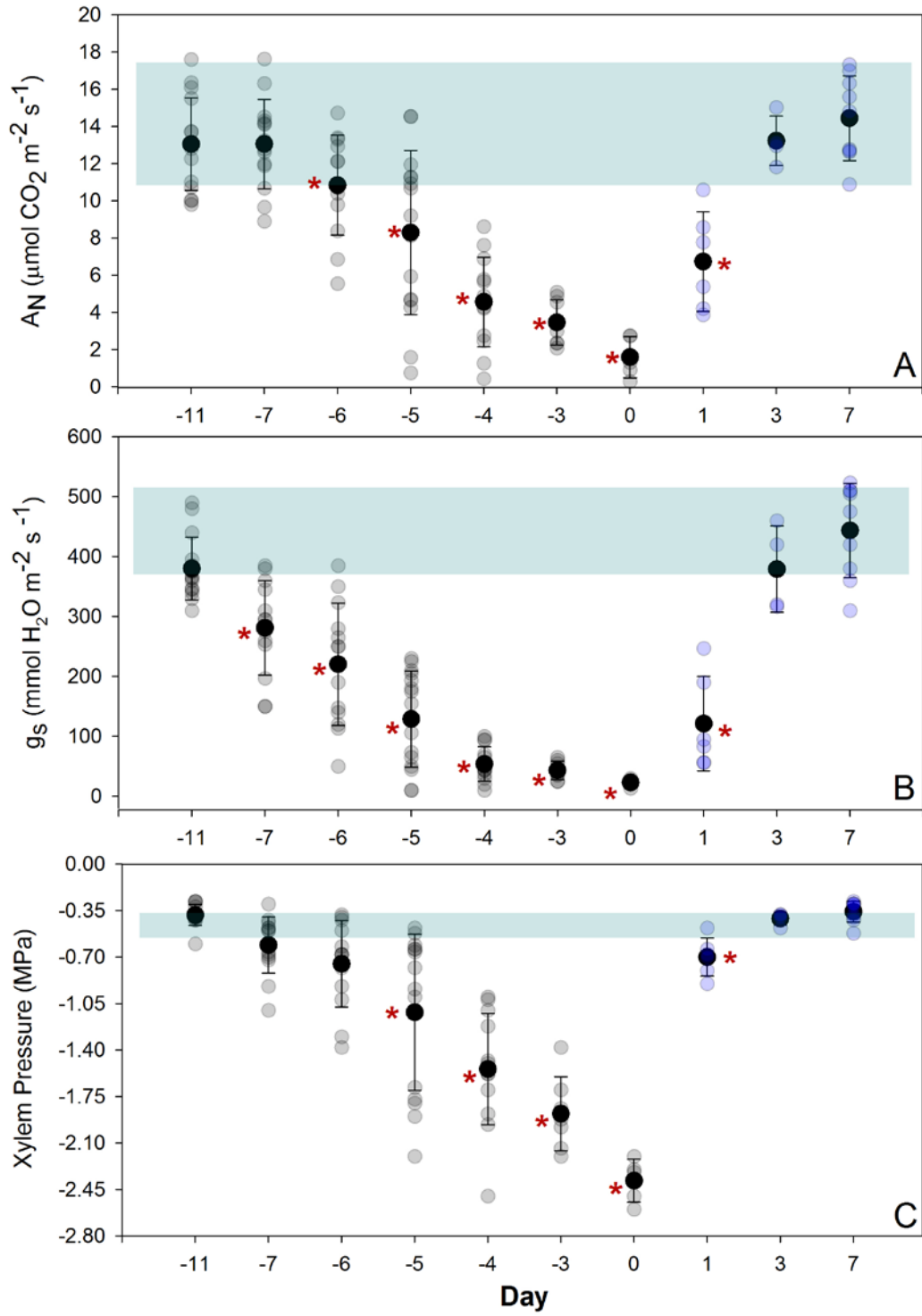
Figure 5

773   **Figure 6**

774

775
776

777 **Figure 7**

778
779